METEOROLOGICAL VISUAL RANGE UNDER HUGE AEROSOL OVERBURDEN

A.S. Ginzburg

Institute of Atmospheric Physics, USSR Academy of Sciences, Moscow
Received January 6, 1989

In this paper it is shown that under conditions of huge effluents of strongly absorbing aerosol in the lower layers of the atmosphere the meteorological visual range depends not only on the aerosol content along the line of sight, but also on the vertical strength of the aerosol layer since it can strongly diminish the illumination of the ground atmospheric layer, so that the threshold contrast becomes important. This interrelationship allows one to assess the strength of an aerosol effluent provided the optical properties of the aerosol and the meteorological visual range are known.

Usually, the decrease of the Illumination of the lower atmospheric layer due to the extinction of radiation by aerosol is not taken into account when estimating the meteorological visual range when daytime conditions. In fact, it is quite natural because even in dense fogs within the visual range of about 50 m, the illumination of the underlying surface decreases by not more than 10 times, while the threshold of the sensitivity of the eye practically does not change[1–7]. A different situation occurs under the conditions when huge effluents of strongly absorbing aerosol are observed with vertical optical depth $\tau \gg 1$ and photon survival probability $\omega \leq 0.9$ ($\tau = (\alpha + \tau)h$; $\omega = \tau(\alpha + \tau)$, where h is the geometrical thickness of the layer, and τ and α are the volume scattering and absorption coefficients of the aerosol). Under these conditions the total intensity of solar radiation F_Σ and, consequently the illuminance τ of the underlying surface decreases not by just one but by two or three orders of magnitude compared to the case of clouds or fogs. The threshold of the sensitivity of the human eye is practically constant for illuminance $J > 1$lux, but rapidly increases at lower illumination. This makes the standard technique for estimating atmospheric turbidity using the visual range value inapplicable under these conditions.

Some remarks concerning the basic relationships are given below. Thus, the meteorological visual range s is defined as the range at which a black screen is discernible on the sky background near the horizon

$$s = \frac{1}{\varepsilon} \ln \frac{1}{k}, \qquad (1)$$

where $\varepsilon = \alpha + \tau$ is the volume extinction coefficient along the path, and k is the value of the threshold contrast discernible by the human eye. With increasing turbidity of the atmosphere a black screen becomes invisible at $k = 0.01 \div 0.02$ (the disappearance threshold), while in the case of increasing transparency of the atmosphere the detection threshold is $k = 0.03$ (Refs. 1, 2, 4, 6). If the type and location of an object are unknown beforehand, the recognition threshold κ can reach the value of 0.05 to 0.07 (Ref. 4, 7). As has already been mentioned, the value k is practically independent of illumination conditions and hence Eq. (1) can be rewritten in the form

$$s = \tau_*/\varepsilon \qquad (2)$$

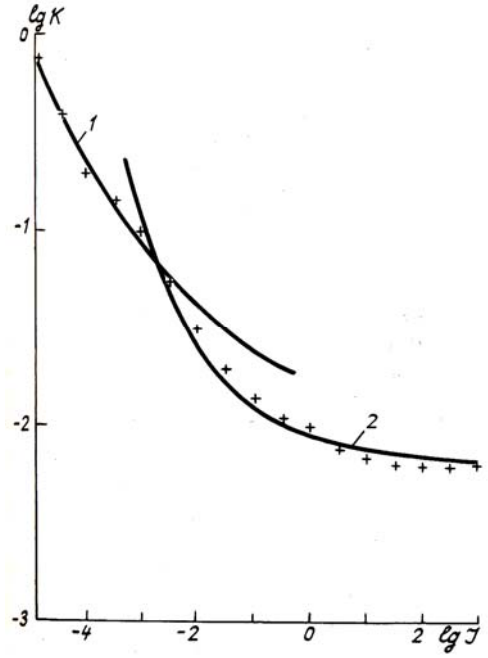

FIG. 1. The threshold of the sensitivity of the human eye according to Ref. 8 and approximation curves for the twilight (1) and daytime illumination.)

The value τ_*/ε varies from 3.0 to 4.0 depending on the value of the threshold contrast $\tau_* = -\ln k$ chosen, and for the commonly used value $k = 0.02$, $\tau_* = 3.9$

(Ref. 4, 7). This τ_* value characterizes the minimal optical depth $\tau_* = \varepsilon \times s$ at which a black screen becomes invisible. It becomes discernible again upon decrease τ_* to ~ 3.

The behavior of the eye sensitivity threshold, with decrease of the illuminance of a fixed object sufficient for its detection with a 50% confidence level during a long observation has been quite well studied under the laboratory conditions[1,5,8]. These values of k are presented in Fig. 1 for objects with angular dimensions less than 6° and brighter than the background. Naturally, they are much lower than values of k for a black screen under natural conditions also shown in Fig. 1 according to Refs. 1, and 8. The latter data clearly reveal the transition from daytime to nighttime (twilight) vision at an illuminance level of $J < 0.1$lux. For illuminance values corresponding to daytime conditions lg$k$ is practically independent of lg$J$. Whereas under lower illumination corresponding to sunset on a cloudy day ($J \sim 10$lux) the sensitivity threshold begins to grow with lg$K$, increasing approximately exponentially with decrease of lg$J$. At the point lg$J \approx -2.75$ a the point optional bend in the curve occurs and the rate of increase of lg$k$ decreases. It is obvious that for such illuminances ($J \approx 10^{-1}$lux) the transition from the daytime to twilight vision occurs. Both portions of the lg$k$ dependence on lg$J$ can be well approximated by the following expression

$$\lg k = b_1 + b_2 \exp[-b_3(\lg J + 2.75)], \quad (3)$$

where $b_1 + b_2 = -1.15$, which corresponds to the value lg$k$ at lg$J = -2.75$. In the case of completely twilight vision and a brighter object $b_1 = -2.25$, $b_2 = 1.1$, and the value depends on the duration of observations and normally is 0.25 to 0.3. In the region lg$J > -2.75$, b_1 is equal to lg$k$ for daytime illuminance while the sum $b_1 + b_2$ is conserved. In this region the values of b_1, b_2, and b_3 all depend on the duration of the observations. Thus for a short observation they are –2.20, 1.01, and –0.30, respectively, while for an infinite observation time they are –2.55, 1.10, and –0.70.

In the region of illuminance values $J < 1$lux, which is important for the applications discussed below, one can use a linear approximation for the dependence of lg$k$ on lg$J$

$$\lg k = c_1 + c_2 \lg J, \quad (4)$$

where, according to Ref. 8, $c_1 \approx -2.4$ to –2.5, and c_2 varies from –0.4 to –0.5, the latter (c_2) depending on the duration of the observation, and according to Ref. 7 $c_1 = -0.8$ and $c_2 = -0.2$. The first pair of these coefficients is applicable to illuminances from 10^{-5} to 10^{-1}lux under the laboratory conditions, while the second is used for the evaluation of the meteorological visual range under natural conditions in the illuminance interval from 10^{-4} to 10^3lux (Fig. 2).

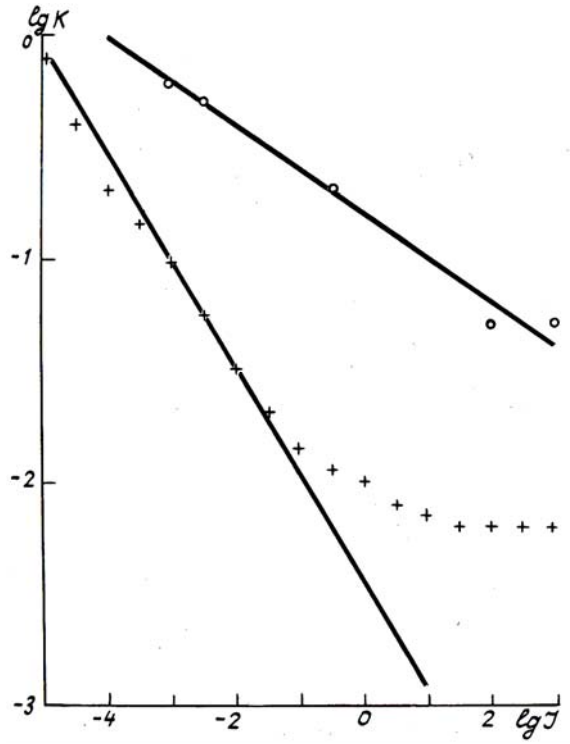

FIG. 2. The threshold of the sensitivity of the human eye sensitivity according to Ref. 8 (1) and Ref. 7 (2) under laboratory and natural conditions, respectively, and the approximate curves (straight lines) for twilight.

Note that at $J = 10^3$ the second approximation yields the value $k = 0.02$, which corresponds to the threshold of the standard eye sensitivity during daytime. This very approximation will be used below.

The illuminance of the Earth's surface J(lux) is determined by the amount of total (i.e. direct plus scattered) solar radiation reaching the surface F_Σ(W/cm^2). According to Ref. 7 J and F_Σ are related by the simple expression

$$J \approx 100\ F_\Sigma. \quad (5)$$

The value F_Σ in turn is determined as follows

$$F_\Sigma = I\ \mu_0\ T(\tau,\ \mu_0), \quad (6)$$

where $I = 650$ W/cm^2 is the value of the solar constant for visible light, μ_0 is the cosine of the Sun's zenith angle, and $T(\tau, \mu_0)$ is the total transmission of the overlying atmospheric layer. In the case of large optical depths one can use the expressions of the asymptotic theory of radiation transfer to estimate the transmission[9], and in presence of strong absorption ($\omega < 0.9$) one can use the expressions suggested in Ref. 10 for calculating the total radiation flux at the lower boundary of a strongly absorbing aerosol layer. For $\tau \gg 1$ and $\omega < 0.9$ both approaches give

$$T(\tau, \mu_0)=K(\mu_0)\times\exp(-r(\mu_0)\times\tau). \quad (7)$$

In the asymptotic theory $K(\mu_0)$ is the limb darkening[9], and $r(\mu_0) = \sqrt{3(1-g\omega)(1-\omega)}$. In the expression for $T(\tau, \mu_0)$ derived in Ref. 11 $K(\mu_0) = 1$ and

$$r(\mu_0) = (1 - \omega \sqrt[4]{g})/\mu_0. \quad (8)$$

Let us now assume that the near-ground atmospheric layer of height h is uniformly filled with light-absorbing aerosol of known optical properties, i.e., volume scattering coefficient, photon survival probability, and mean scattering cosine. Using a combination of the relationships (2), (4), and (7), one can determine the meteorological visual range s near the ground from the known value h, or, vice versa from the value s measured near the ground one can determine the vertical depth of an aerosol layer. If the mass coefficient (ε_m) of aerosol extinction is known but not the volume coefficient, these relationships determine, at a given visual range, the column mass of the aerosol instead of the geometrical depth.

Consider now the dependence of the volume extinction coefficient and the column mass of the aerosol on the value of the visual range at the lower boundary of the aerosol layer. Successively substituting expression (8) into (7), (7) into (6), (6) into (5), (5) into (4), and (4) into (1), one obtains the following expression

$$\tau = \varepsilon\times h = \varepsilon_m \times m \quad (9)$$

relating the vertical optical depth of the layer and the visual range in its lower part. Approximations (4) and (7) mentioned above were chosen to yield a very simple relationship between ε and s

$$\varepsilon = \tau_*/(ah+s). \quad (10)$$

Here the coefficient a characterizes the ratio of extinctions along vertical and horizontal directions.

Let us now use the above-obtained expressions to estimate the extinction coefficient and mass of the aerosols in the lower layers of the atmosphere after a heavy infusion of smoke from large fires of natural or anthropogenic origin[10,12,13]. The optical properties of smokes strongly depend on the content f of pure carbon soot in their particles. In many articles[12–13] a simple relation between the mass extinction coefficient and the probability of photon survival per unit volume of smoke is used. In the construction of this relation, it is assumed that the scattering coefficient does not depend on the soot content of the smoke particles and is given by $\sigma_m = 3.5\ m^2/g$, but the absorption coefficient is proportional to f and is given by $a_m = 10f$. As a result, one has

$$\varepsilon_m = 3.5+10f \quad (11)$$

and

$$\omega_m = 3.5 \quad (12)$$

In the light transmitted through forest smokes the values of и and f are 0.9 and 0.05, respectively, while for pure soot particles $f = 1$ and $\omega \approx 0.25$.

Figure 3 presents ε as a function of the meteorological visual range for the case of homogeneous smoke layers, 2 km thick, at different f values; the straight line corresponds to expression (2). The corresponding values of the aerosol column mass determined by the formula

$$m = \varepsilon h/\varepsilon_m \quad (13)$$

are also shown in this figure.

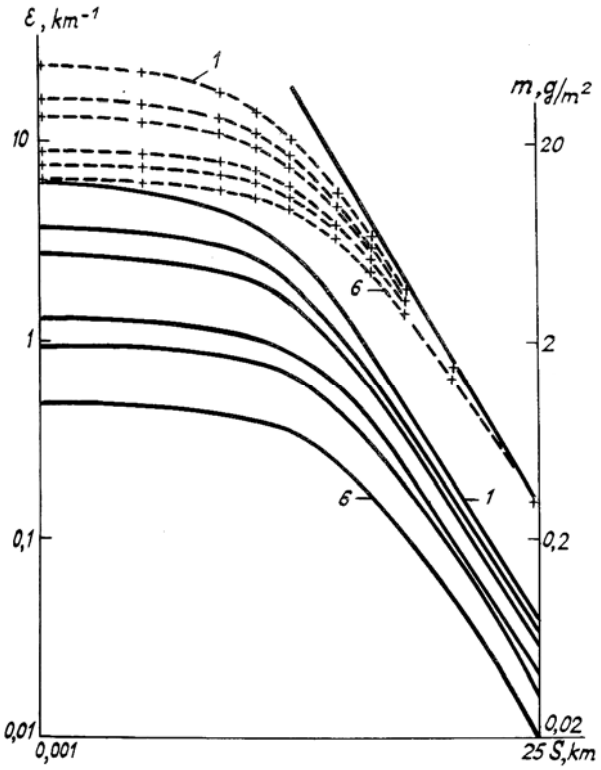

FIG. 3. Volume extinction coefficient $\varepsilon(km^{-1})$ (dashed lines) and column density of a smoke layer equal to 2 km in thickness $m(g/m^2)$ (solid lines) as functions of the meteorological visual range s at different f values: curve 1 (f = 0.05); 2 (f = 0.1); 3 (f = 0.15); 4 (f = 0.35); 5 (f = 0.5); 7 (f = 1.0); a straight line represents the Kohschmieder formula.

One can see from Fig. 3 that in a clear atmosphere the relationship between ε and the meteorological visual range is described by the Kohschmieder formula (2). With decrease of s, the role of the decrease of the illuminance grows, and when $s \ll ah$, the extinction coefficient and aerosol mass are already independent of

the meteorological visual range. It is natural, that the value of the extinction coefficient relevant to the given (small) visual range decreases with increase of h. This is illustrated by Fig. 4, where the dependence of ε on s is presented for the case of $f = 0.35$ and $\omega = 0.7$ for different layer thicknesses h.

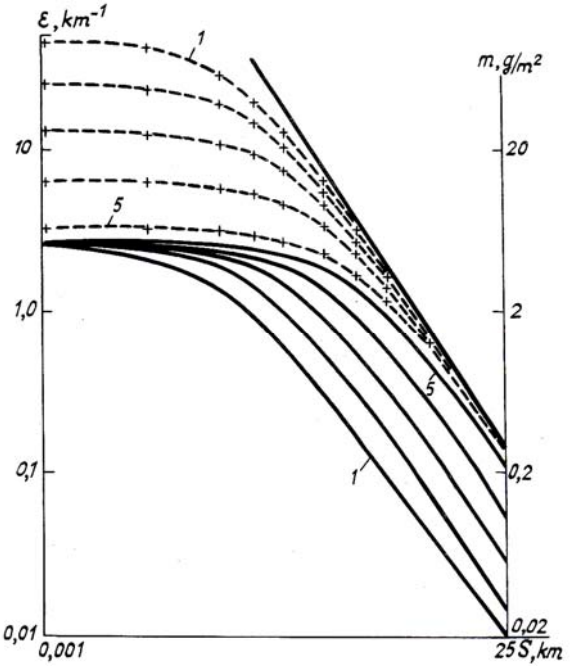

FIG. 4. The same data as in Fig. 3 but at $f = 0.15$, the height of the upper boundary of the layer being 0.5 (curve 1), 1.0 (2), 2 (3), 4.0 (4) and 8 km (curve 4).

Note that such parameters are typical for a mixture of wood and urban smoke[12,18]. It is readily seen from Fig. 4, that ε and m behave differently in clear and smoked atmospheres. In particular, it is seen that at small visual range values m is independent of s. The maximum values of ε and m at the smallest, yet meaningful values of s (~ 1 m), are presented in the Table for $h = 2$ km and for different types of smokes.

TABLE 1.

The fraction f of pure carbon in smoke particles, the single scattering albedo ω, the volume extinction coefficient ε [km^{-1}] and the corresponding smoke mass m [g/m^2] in a column of homogeneous layer 2 km thick.

f	0.05	0.1	0.15	0.35	0.5	1.0
ω	0.875	0.778	0.700	0.500	0.412	0.259
ε	24.4	16.9	13.6	9.0	7.8	6.4
m	12.2	7.5	5.4	2.6	1.8	0.95

Let us use the results obtained here to estimate the smoke yield during the huge forest fires in Siberia during the summer of 1915. The visibility during this disaster was strongly diminished. According to Refs. 19 and 20 the visual range did not exceed 100 m over an area of 2.8×10^6 km^2, while over 2.2×10^6 km^2 the visual range was 100 to 25 m, and over 1.8×10^6 km^2 it was 25 to 4 m. For each category we may assign a nominal visual range be $s_1 = 100$ m, $s_2 = \sqrt{100 \times 25} = 50$ m and $s_3 = \sqrt{25 \times 4} = 10$ m. For the light transmitted through forest smoke one obtains $m_1 = 8$, $m_2 = 9.5$, and $m_3 = 12$ g/m^2, which yields about 60 Tg (1 Tg = 10^{12} g) of smoke. It is obvious that not all observations were conducted simultaneously, therefore the above estimate must be considered as the upper boundary of the possible emission of smoke during the great Siberian fires during the summer of 1915[21–24]. During such great fires the soot content in the smoke can be much larger than 0.05. If one takes $f = 0.1$ and $\omega \approx 0.8$, the estimated value of the smoke emission decreases to 40 Tg and at $\omega \approx 0.7$ (the case of dry wood burnt under the laboratory conditions[15,16]) the smoke emission does not exceed 30 Tg.

A lower boundary for the total mass of smoke can be obtained, taking into account the whole fire area of 140 km^2 (Refs. 19 and 20). According to Ref. 12, forest fires can produce ~ 17 Tg of smoke from such an area. On the other hand, it was noted in Refs. 19 and 20 that in 1915 one half of the forest mass of this area or about 1.6×10^9 m^3 of pine tree wood was completely burnt. At a density of 0.5 tons/m^3 and 3% smoke mass yield[21] one obtains 24 Tg. Thus, the value of 20 Tg can obviously be taken as a lower limit since such calculations do not take into account the burning of fallen trees, surface layer, or smoke from small-scale fires.

Thus, different estimates of the smoke mass yield during huge fires give comparable results. This technique for estimating the mass of huge aerosol emissions into the atmosphere can be used not only for smokes but for other light-absorbing aerosols as well.

REFERENCES

1. W.E.K. Middleton, *Vision through the Atmosphere* (Univ. Press, Toronto, 1952).
2. V.V. Sharonov, *Light and Colour* (Fizmatgiz, Moscow, 1961).
3. N.G. Boldyrev and O.D. Barteneva, Trudy GGO, No. 118, 3 (1961).
4. V.A. Gavrilov *Vision through the Atmosphere* (Gidrometeoizdat, Leningrad, 1966).
5. E. McCartney, *Optics of the Atmosphere* (Mir, Moscow, 1979).
6. V.A. Kovalev, *Visibility in the Atmosphere and its Determination* (Gidrometeoizdat, Leningrad, 1988).

7. L.T. Matveev, *A Course in General Meteorology. Atmospheric Physics* (Gidrometeoizdat, Leningrad, 1984).
8. H.R. Blackwell, J. Opt. Soc. Amer., **36**, No. 11, 624 (1946).
9. I.N. Minin, *The Theory of Radiation Transfer in Planetary Atmospheres* (Nauka, Moscow, 1988).
10. G.S. Golitsyn and A.S. Ginzburg, Tellus, **37B**, No. 3, 173 (1985).
11. A.S. Ginzburg and I.N. Sokolik, Izvestiya Akad. Nauk SSSR, Ser. Fizika Atmosfery i Okeana (to be published).
12. P.J. Crutzen, I.E. Galbally, and C. Bruhl, Climatic Change, **6**, No. 3, 323 (1984).
13. E.M. Patterson, C.K. McMahon and D.E. Ward, Geophys. Res. Letters, **13**, 129 (1986).
14. G.S.Golitsin, A.H. Shukurov, A.S. Ginzburg, et al., Izvestiya Akad. Nauk SSSR, Ser. Fizika Atmosfery i Okeana, **24**, No. 3, 227 (1988).
15. A.V. Andronova., E.M. Kostina, A.S. Kutov, et al., ibid., 235.
16. P.P. Anikin and A.H. Shukurov Izvestiya Akad. Nauk SSSR, Ser. Fizika Atmosfery i Okeana, **24**, No. 3, 244 (1988).
17. I.N. Sokolik, Ibid., 274.
18. V.B. Shostakovich, *Forest Conflagrations in Siberia in 1915*, Izvestiya Vost.-Sib. Otd. Rossiiskogo Geograf. Obshchestva, **47**, 1 (1924).
19. V.B. Shostakovich, *Forest Conflagrations in Siberia*, J. Forestry, **23**, 365 (1925).
20. A.S. Ginzburg and G.S. Golitsyn, *Comparative Analysis of Natural and Nuclear Conflagrations* Proceedings of the All-Union Conference on Problems of Peace and Prevention of Nuclear War, May 26–29, Moscow, (1986).
21. R. Seitz, Nature, **323**, 116 (1986).
22. N.N. Vel'tishchev, A.S. Ginzburg, and G.S. Golitsyn, Izvestiya Akad. Nauk SSSR, Ser. Fizika Atmosfery i Okeana, **24**, No. 3, 296 (1988).